

# Oncostatin M produced in Kupffer cells in response to PGE<sub>2</sub>: possible contributor to hepatic insulin resistance and steatosis

Janin Henkel<sup>1</sup>, Daniela Gärtner<sup>1</sup>, Christoph Dorn<sup>2</sup>, Claus Hellerbrand<sup>2</sup>, Nancy Schanze<sup>1</sup>, Sheila R Elz<sup>1</sup> and Gerhard P Püschel<sup>1</sup>

Hepatic insulin resistance is a major contributor to hyperglycemia in metabolic syndrome and type II diabetes. It is caused in part by the low-grade inflammation that accompanies both diseases, leading to elevated local and circulating levels of cytokines and cyclooxygenase (COX) products such as prostaglandin E<sub>2</sub> (PGE<sub>2</sub>). In a recent study, PGE<sub>2</sub> produced in Kupffer cells attenuated insulin-dependent glucose utilization by interrupting the intracellular signal chain downstream of the insulin receptor in hepatocytes. In addition to directly affecting insulin signaling in hepatocytes, PGE<sub>2</sub> in the liver might affect insulin resistance by modulating cytokine production in non-parenchymal cells. In accordance with this hypothesis, PGE<sub>2</sub> stimulated oncostatin M (OSM) production by Kupffer cells. OSM in turn attenuated insulin-dependent Akt activation and, as a downstream target, glucokinase induction in hepatocytes, most likely by inducing suppressor of cytokine signaling 3 (SOCS3). In addition, it inhibited the expression of key enzymes of hepatic lipid metabolism. COX-2 and OSM mRNA were induced early in the course of the development of non-alcoholic steatohepatitis (NASH) in mice. Thus, induction of OSM production in Kupffer cells by an autocrine PGE<sub>2</sub>-dependent feed-forward loop may be an additional, thus far unrecognized, mechanism contributing to hepatic insulin resistance and the development of NASH.

*Laboratory Investigation* (2011) 91, 1107–1117; doi:10.1038/labinvest.2011.47; published online 25 April 2011

**KEYWORDS:** cyclooxygenase; cytokine; hepatic steatosis; NASH; suppressor of cytokine signaling (SOCS); type II diabetes (T2DM)

The metabolic syndrome and type II diabetes are major health problems worldwide, with a steadily increasing prevalence. Hepatic insulin resistance is recognized as a major contributor to the pathologically elevated fasting blood glucose levels in these disorders. Both are often accompanied by non-alcoholic fatty liver disease (NAFLD), with pathological conditions ranging from 'bland' steatosis to non-alcoholic steatohepatitis (NASH), which can progress to significant fibrosis and ultimately may lead to cirrhosis. Interestingly, there is a close correlation between hepatic steatosis and insulin resistance. The low-grade chronic inflammation that can be found systemically and locally in the liver also contributes in part to hepatic insulin resistance.<sup>1</sup> In the liver, any systemic or local inflammation elicits a response that involves a complex intercellular communication between parenchymal and non-parenchymal liver cells involving

locally produced cytokines and prostanoids.<sup>2</sup> Cytokines and prostanoids released from non-parenchymal liver cells, primarily resident liver macrophages (Kupffer cells), modulate the function of parenchymal cells in a paracrine mode but may also alter their own function in an autocrine mode. Thus, tumor necrosis factor- $\alpha$  (TNF- $\alpha$ ), interleukin (IL)-1 $\beta$  and IL-6 released from Kupffer cells enhance the positive acute-phase response in hepatocytes. Prostaglandins released from Kupffer cells can modulate hepatic glucose output<sup>3,4</sup> and can attenuate the induction of positive acute-phase proteins by IL-6.<sup>5</sup> In an autocrine feed-back loop, prostaglandin E<sub>2</sub> (PGE<sub>2</sub>) released from Kupffer cells can inhibit TNF- $\alpha$ <sup>6</sup> and IL-6 production<sup>7,8</sup> but it has also been reported to enhance IL-6 production by Kupffer cells in another study.<sup>9</sup> TNF- $\alpha$  and IL-6 are known to elicit hepatic insulin resistance,<sup>10</sup> and recent evidence clearly suggests that Kupffer

<sup>1</sup>Universität Potsdam, Institut für Ernährungswissenschaft, Biochemie der Ernährung, Nuthetal, Germany and <sup>2</sup>Department of Internal Medicine I, University Hospital Regensburg, Regensburg, Germany

Correspondence: Professor GP Püschel, MD, Universität Potsdam, Institut für Ernährungswissenschaft, Abt. Biochemie der Ernährung, Arthur-Scheunert-Allee 114-116, D-14558 Nuthetal, Germany.

E-mail: gpuesche@rz.uni-potsdam.de

Received 22 September 2010; revised 10 January 2011; accepted 27 January 2011

cells play a central role in the development of hepatic insulin resistance.<sup>11</sup> We have recently shown that PGE<sub>2</sub> can cause insulin resistance in hepatocytes by a mechanism distinct from but synergistically with IL-6.<sup>12</sup> In the more complex situation of the intact liver, PGE<sub>2</sub> might not only affect hepatic insulin resistance via direct action on hepatocytes but also by modulating the release of other signaling molecules from Kupffer cells. In order to investigate this possibility, we studied the effect of PGE<sub>2</sub> on the cytokine production in Kupffer cells. We show that PGE<sub>2</sub> enhanced the production of oncostatin M (OSM) in Kupffer cells and identified OSM as a so far unrecognized mediator of insulin resistance and possible contributor to the development of steatosis and inflammation in a murine NASH model.

## MATERIALS AND METHODS

### Materials

Narcoreen was purchased from Merial GmbH (Hallbergmoos, Germany). Percoll™ PGE<sub>2</sub> was purchased from Alexis (Grünberg, Germany); IL-6 was obtained from Strathmann Biotec AG (Hamburg, Germany). Recombinant mouse OSM was purchased from Miltenyi Biotec (Bergisch-Gladbach, Germany). Antibodies against signal transducer and activator of transcription 3 (STAT3), pSTAT3, Akt and pAkt were purchased from Cell Signaling Technology (Frankfurt am Main, Germany) and against rat OSM from Santa Cruz Biotechnology (Heidelberg, Germany). SuperSignal West Pico Chemiluminescent Substrate was obtained from Pierce (Rockford, IL, USA).

### Animals

Male Wistar rats (200–300 g) were purchased from Charles River (Sulzfeld, Germany) and kept on a 12-h day/night rhythm with free access to water and a standard 1326 rat diet (altromin). The principles of laboratory animal care were followed. Treatment of the animals followed the German animal protection laws and was performed with permission of the state animal welfare committee.

### Murine Models of Hepatic Steatosis and Hepatic Inflammation

Male BALB/c mice were purchased from Charles River Laboratories at 6 weeks of age and housed in a 22 °C controlled room under a 12 h light/dark cycle with free access to food and water. After 1 week of acclimatization, mice were divided into three groups ( $n=6$  each) and fed either a control diet, a high-fat diet (HFD) containing 30% lard, or a NASH-inducing diet containing 30% lard, 1.25% cholesterol and 0.5% sodium cholate.<sup>13,14</sup> All chows were prepared by Ssniff (Soest, Germany). After 12 weeks of feeding, animals were killed. Liver tissue was immediately snap frozen and stored at –80 °C for subsequent analysis.

### Hepatocyte Preparation and Cultivation

Density gradient-purified hepatocytes were prepared without the use of collagenase as described previously.<sup>15,16</sup> Hepatocytes were plated on 35-mm diameter tissue culture plates (10 mg/plate,  $1 \times 10^6$  cells/plate) in M199 containing 1% (v/v) antibiotics (10 U/ $\mu$ g penicillin, 10  $\mu$ g/ $\mu$ l streptomycin), 100 nM dexamethasone, 0.5 nM insulin and, for the first 4 h of culture, 4% (v/v) newborn calf serum. Experimental treatments were performed after 44 h of culture in M199 containing 1% (v/v) antibiotics and 100 nM dexamethasone.

### Kupffer Cell Preparation and Cultivation

Kupffer cells were isolated from rat livers by two-step collagenase-pronase perfusion and subsequently purified by a discontinuous nycodenz gradient as described in detail previously.<sup>6</sup> They were cultured in RPMI medium containing 30% newborn calf serum for 72 h before the experiment. Peritoneal macrophages were isolated by peritoneal lavage with phosphate-buffered saline (PBS) and cultured as described for Kupffer cells.

### Immunochemical Protein Analysis

Rat hepatocytes and Kupffer cells were cultivated as described and incubated for the times indicated with 10  $\mu$ M PGE<sub>2</sub>, 100 ng/ml IL-6 or 10 ng/ml OSM, as indicated. In some experiments, cells were subsequently stimulated with 10 nM insulin for the times indicated. Cells were washed with ice-cold PBS and frozen in liquid nitrogen. Cell lysates were prepared by addition of 100  $\mu$ l of lysis buffer per culture plate (20 mM Tris pH 7.4, 150 mM NaCl, 1 mM EDTA, 1 mM EGTA, 1% (v/v) Triton X-100, 2.5 mM sodium pyrophosphate, 1 mM  $\beta$ -glycerolphosphate, 50 mM NaF) with protease inhibitors and 1 mM sodium orthovanadate. The detached cells were disrupted by sonication and insoluble material was removed by centrifugation (10 000 g, 15 min, 4 °C). Protein content was determined by the method of Bradford.<sup>17</sup> Kupffer cell supernatants were precipitated with 6 ml acetone per 1 ml supernatant overnight at –20 °C, centrifuged (5000 r.p.m., 1 min), dried and dissolved in lysis buffer to yield a 29-fold concentrated solution. Cell lysates with an equal protein content or concentrated Kupffer cell supernatants were boiled for 5 min in Laemmli buffer, resolved by SDS-PAGE, and transferred to a polyvinylidene difluoride (PVDF) membrane.<sup>18</sup> After transfer, membranes were blocked in 5% nonfat dry milk dissolved in 20 mM Tris, 136 mM NaCl and 0.1% (v/v) Tween (TBS/Tween) for 1 h at room temperature, then membranes were incubated with the first antibody in TBS/Tween containing 5% nonfat dry milk or 5% bovine serum albumin overnight at 4 °C. Membranes were washed three times with TBS/Tween before they were incubated with horseradish-peroxidase-conjugated anti-mouse or anti-rabbit IgG for 2 h at room temperature. Visualization of immune complexes was performed using chemoluminescence reagent.

Rat IL-6 was determined in Kupffer cells supernatants with a rat IL-6-specific commercial ELISA according to the instructions of the manufacturer (R&D Systems, Minneapolis, MN, USA).

### Quantitative PCR

Rat hepatocytes or Kupffer cells were cultivated as described and incubated for the times indicated with or without 10  $\mu$ M PGE<sub>2</sub>, 100 ng/ml IL-6 or 10 ng/ml OSM, as specified. In some cases, cells were subsequently stimulated with 10 nM insulin for 120 min. Cells were washed with ice-cold PBS and frozen in liquid nitrogen. RNA was isolated using the SV Total RNA Isolation System (Promega, Madison, WI, USA). cDNA was synthesized from purified RNA. RNA, 500 ng Oligo(dT)<sub>12–18</sub> and 200 ng random hexamer primer were incubated at 70 °C for 5 min. Subsequently, the samples were kept on ice and 5  $\times$  RT buffer and 1 mM dNTP mix were added. After 5 min of incubation at 37 °C, 200 U of RevertAid™ H Minus M-MuLV reverse transcriptase (MBI Fermentas GmbH, St Leon-Rot, Germany) was added and samples were kept at 42 °C for 90 min, followed by 10 min at 70 °C. The total reaction volume was 20  $\mu$ l. Hot start real-time PCR for the quantification of IL-6, OSM, suppressor of cytokine signaling 3 (SOCS3), glucokinase, carnitine palmitoyl transferase 1 (CPT1), microsomal triglyceride transfer protein (MTP), Apolipoprotein B (ApoB) and  $\beta$ -actin as a housekeeping gene was carried out in triplicates in a reaction mixture of 2  $\times$  Maxima™ SYBP Green qPCR Master Mix (MBI Fermentas GmbH), 250 nM forward and reverse oligonucleotides (MWG BiotechAG, Ebersberg, Germany), and 0.3  $\mu$ l cDNA in a total volume of 10  $\mu$ l. The following oligonucleotides were used as forward and reverse primers, respectively: 5'-TGA CAGCCACTGCCTTCCCT-3' and 5'-ACGGAAGTCCAGAA GACCAGAGCA-3' for IL-6; 5'-GGGCTCAGCCTCCACCG AGA-3' and 5'-TGGCGTGCACAGTGCTCAGG-3' for OSM (rat); 5'-GGCACTGGCCAATCGTGGCT-3' and 5'-GCCGG GCACTGTCCAGCTTT-3' for OSM (mouse); 5'-GACCTT CAGCTCCAAGAGCGAGTA-3' and 5'-CGCCCCAGAATA GATGTAGTAAGC-3' for SOCS3; 5'-GCCGTGCCTGTGA AAGCGTGTC-3' and 5'-CCACCCGTAGCAGCAGAATAGG TC-3' for glucokinase; 5'-CCAAGCTGTGGCCTTCCAGT-3' and 5'-GGACGCCGCTCACAAATGTTTC-3' for CPT1; 5'-AGA CTCCAGCCTCACTGGAA-3' and 5'-TGCAGCCTTCATT CTGACAC-3' for MTP; 5'-CAGGCTGATGCTGTTTGGAA-3' and 5'-CTGAGGGATTTGGGATCAGA-3' for ApoB as well as 5'-CCCTAAGGCCAACCGTGAAAAGATG-3' and 5'-AGGT CCCGGCCAGCCAGGTCCAG-3' for  $\beta$ -actin. qPCR was performed with an initial DNA denaturation and enzyme activation step at 95 °C for 3 min, followed by 52 cycles of denaturation at 95 °C for 20 s, annealing at 57–60 °C for 20 s and extension at 72 °C for 30 s in a CFX™ Thermal Cycler (Bio-Rad, München, Germany). Data were expressed as CT values (the cycle number at which logarithmic PCR plots cross a calculated threshold line). Gene of interest RNA expression was normalized to  $\beta$ -actin by the formula:  $N\text{-fold induction} = 2^{(CT \text{ gene of interest (control)} - CT \text{ gene of$

interest (stimulated sample))/2^{(CT \beta\text{-actin (control)} - CT \beta\text{-actin (stimulated sample))}. Expression of murine IL-6, cyclooxygenase 1 (COX-1) and COX-2 mRNA was analyzed with the QuantiTect Primer Assays according to the manufacturer's instructions (Qiagen, Hilden, Germany) using 18s RNA with the primer pair 5'-AAACGGCTACCACATCC AAG-3' and 5'-CCTCCAATGGATCCTCGTTA-3' as a reference gene.

## RESULTS

### STAT3 Phosphorylation in Hepatocytes by Kupffer Cell-Conditioned Medium

We and others have previously shown that PGE<sub>2</sub> and IL-6 interact to modulate the liver's response to inflammation in a complex manner:<sup>5,19</sup> IL-6 is a major mediator of the acute-phase response in hepatocytes. In primary cultures of isolated rat hepatocytes, it increased STAT3 phosphorylation (Figure 1) and thereby enhanced the expression of positive acute-phase proteins (not shown). As previously shown, PGE<sub>2</sub> tended to reduce the IL-6-dependent STAT3 phosphorylation (Figure 1), thereby attenuating the acute-phase response (not shown), although this effect was not significant in the current study. Notably, PGE<sub>2</sub> itself had no influence on the basal STAT3 phosphorylation in isolated hepatocytes (Figure 1). In order to elucidate the impact of PGE<sub>2</sub> on the STAT3 phosphorylation in the more complex situation of the whole liver, in which intercellular communication between Kupffer cells and hepatocytes contributes to the signal generation, hepatocytes were incubated with Kupffer cell-conditioned medium. Kupffer cell-conditioned control medium caused a stronger STAT3 phosphorylation in hepatocytes than the control medium that had no previous contact with Kupffer cells (Figure 1). Apparently, unstimulated Kupffer cells already secreted one or more mediators that caused STAT3 phosphorylation in hepatocytes. STAT3 phosphorylation in hepatocytes by conditioned medium was only slightly enhanced if Kupffer cells were incubated with IL-6 during the conditioning period. Thus, IL-6 most likely neither enhanced the mediator production by Kupffer cells to any significant extent nor did the IL-6 still present in the conditioned medium add to the background STAT3 phosphorylation in the hepatocytes caused by Kupffer cell-conditioned control medium. However, in contrast to unconditioned PGE<sub>2</sub>-containing medium, medium that had been conditioned by Kupffer cells in the presence of PGE<sub>2</sub> increased STAT3 phosphorylation in hepatocytes to a larger extent than IL-6 (Figure 1). The strongest STAT3 phosphorylation was observed with medium conditioned by Kupffer cells in the presence of a combination of IL-6 and PGE<sub>2</sub> (Figure 1). As PGE<sub>2</sub> did not itself cause a STAT3 phosphorylation in hepatocytes, the results indicated that PGE<sub>2</sub> stimulated the release of one or more mediators from Kupffer cells that are capable of stimulating STAT3 phosphorylation in hepatocytes.

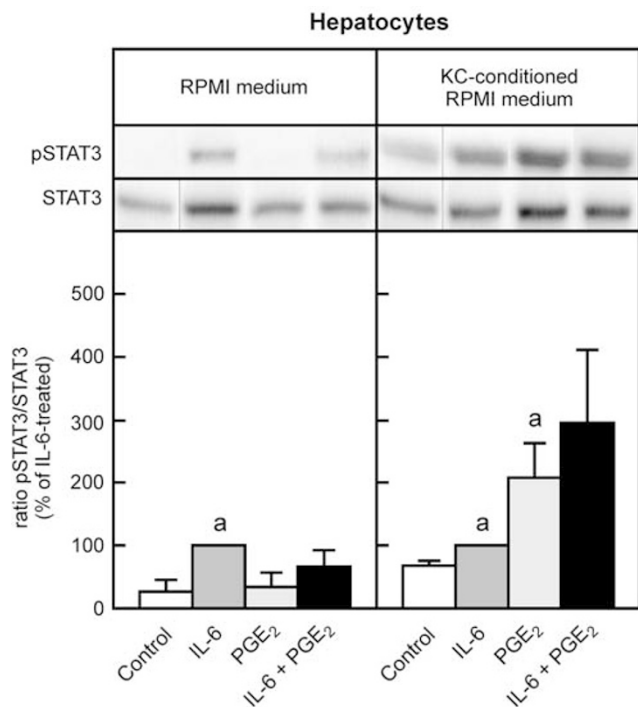


**Figure 1** STAT3 phosphorylation in hepatocytes by IL-6 and an unknown cytokine released from Kupffer cells in response to PGE<sub>2</sub>. Rat hepatocytes were isolated non-enzymatically and highly purified by density gradient centrifugation. They were cultured as detailed in the Materials and methods section for 48 h. Before the experiment, hepatocytes were washed twice with RPMI medium without NCS and preincubated for 30 min with RPMI medium without NCS. Kupffer cells were isolated by a combined pronase/collagenase digestion and purified on a nonlinear nycodenz gradient. They were cultured for 72 h. They were then washed two times with RPMI medium without NCS and incubated for 30 min with RPMI medium without NCS before stimulation with 100 ng/ml human IL-6, 10  $\mu$ M PGE<sub>2</sub> or both for 120 min. Kupffer cell-conditioned medium or unconditioned RPMI medium to which the same stimuli had been added were then applied to the primary cultures of rat hepatocytes. After 360 min, hepatocytes were solubilized in lysis buffer. STAT phosphorylation was determined by western blot analysis with STAT3 and phospho-STAT3-specific antibodies. Values are means  $\pm$  s.e.m. of four independent experiments. The ratio of pSTAT3/STAT3 in hepatocytes treated with IL-6 or Kupffer cell medium conditioned in the presence of IL-6, respectively, was set to 100%. Statistics: Student's t-test for unpaired samples; <sup>a</sup> $P < 0.05$  versus respective control.

### Modulation of Cytokine Production in Kupffer Cells by PGE<sub>2</sub>

It is well known that PGE<sub>2</sub> can modulate the endotoxin-stimulated cytokine production in Kupffer cells. Thus, it inhibited the endotoxin-induced TNF- $\alpha$  production and either inhibited or augmented the endotoxin-induced IL-6 production without affecting the cytokine production in the absence of endotoxin.<sup>6,7,9</sup> In line with these observations, PGE<sub>2</sub> barely affected the IL-6 expression on the mRNA level (Figure 2a) and did not enhance IL-6 secretion from Kupffer cells (Figure 2b). IL-6 caused a slight but not significant increase in IL-6 mRNA. As human IL-6 was used to stimulate Kupffer cells, it was possible to determine the endogenous

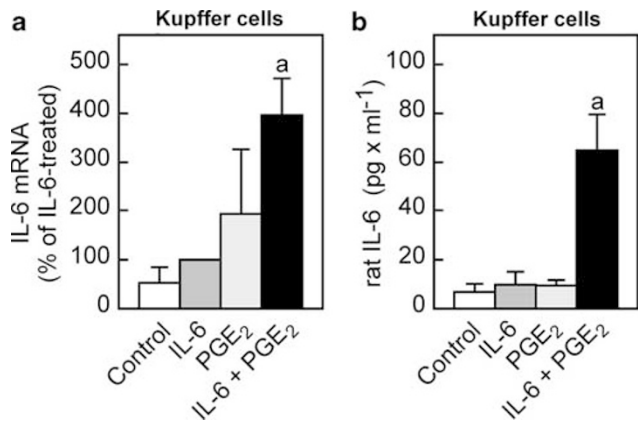


**Figure 2** Induction of IL-6 production in Kupffer cells by the combined stimulation with IL-6 and PGE<sub>2</sub>. Kupffer cells were isolated, cultured and stimulated as detailed in the legend to Figure 1. (a) Cells were lysed in chaotropic buffer and the mRNA was quantified by RT real-time PCR with  $\beta$ -actin as reference gene as described in the Materials and methods section. The IL-6 mRNA level in IL-6-treated Kupffer cells was set to 100%. (b) Rat IL-6 was determined in Kupffer cell-conditioned medium. An ELISA was employed that was highly specific for rat IL-6 and did not crossreact with human IL-6, which was used to stimulate the Kupffer cells. Values are means  $\pm$  s.e.m. of three independent experiments. Statistics: Student's t-test for unpaired samples; <sup>a</sup> $P < 0.05$  versus control.

IL-6 production with an ELISA highly selective for rat IL-6. Human IL-6 did not enhance the endogenous IL-6 production in rat Kupffer cells (Figure 2b). A significant increase in IL-6 mRNA was observed only after a combined stimulation of Kupffer cells with IL-6 and PGE<sub>2</sub>. Under these conditions, a significant amount of rat IL-6 also accumulated in the Kupffer cell supernatant (Figure 2b). Notably, the final concentration of rat IL-6 in the supernatant was about two to three orders of magnitude lower than the amount of human IL-6 added to the cultures. Thus, a PGE<sub>2</sub>-dependent increase in Kupffer cell IL-6 production was apparently not responsible for the STAT3 phosphorylation by Kupffer cell-conditioned media in response to PGE<sub>2</sub>.

### PGE<sub>2</sub>-Dependent Stimulation of OSM Production in Kupffer Cells

Among the cytokines that activate STAT3-dependent signaling pathways, OSM is produced by activated macrophages and thus seemed to be a likely candidate to be produced in Kupffer cells in response to PGE<sub>2</sub>. PGE<sub>2</sub> induced the OSM mRNA approximately sevenfold (Figure 3a). IL-6 affected neither the basal nor the PGE<sub>2</sub>-dependent induction of OSM mRNA. Treatment of Kupffer cells with PGE<sub>2</sub> for 24 h increased the OSM protein content in supernatants approximately five- to six-fold (Figure 3b). IL-6, which left basal OSM formation almost unaffected, did not alter the PGE<sub>2</sub>-dependent OSM induction. Similar results were obtained after 2 h of PGE<sub>2</sub> and/or IL-6 treatment, and the absolute OSM concentration was approximately twofold lower (not shown). Thus, OSM appeared to be a likely candidate

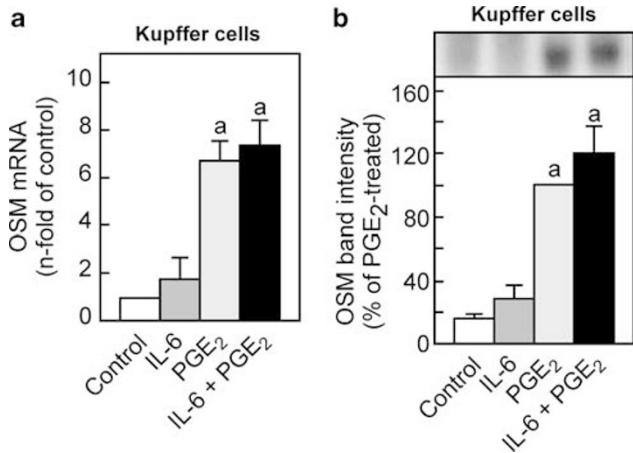


**Figure 3** Induction of oncostatin M production in Kupffer cells by PGE<sub>2</sub>. Kupffer cells were isolated, cultured and stimulated as detailed in the legend to Figure 1. (a) Cells were lysed in chaotropic buffer and the oncostatin M mRNA was quantified by RT real-time PCR with  $\beta$ -actin as reference gene as described in the Materials and methods section. (b) Rat oncostatin M was determined after 24 h culture in Kupffer cell-conditioned medium by western blot analysis. The band intensity in the lane with supernatants of PGE<sub>2</sub>-stimulated cells was set to 100%. Values are means  $\pm$  s.e.m. of three independent experiments. Statistics: Student's *t*-test for unpaired samples; <sup>a</sup>*P* < 0.05 versus control.

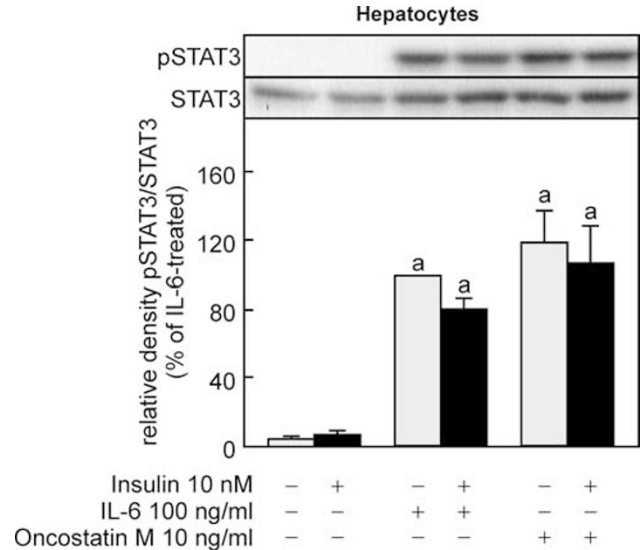


**Figure 4** STAT3 phosphorylation by IL-6 and oncostatin M in rat hepatocytes. Rat hepatocytes were isolated and cultured as described in the legend to Figure 1. After a final medium change, hepatocytes were incubated with IL-6 or oncostatin M for 330 min and subsequently without a further medium change with insulin for 15 min, as indicated. Cells were shock frozen, solubilized in lysis buffer and STAT3 phosphorylation was determined by western blot analysis with phospho-specific antibodies. The density ratio of pSTAT3/STAT3 of IL-6-treated hepatocytes was set to 100%. Values are means  $\pm$  s.e.m. of three independent experiments. Statistics: Student's *t*-test for unpaired samples; <sup>a</sup>*P* < 0.05 versus control.

that caused STAT3 phosphorylation in hepatocytes by Kupffer cell media conditioned in the presence of PGE<sub>2</sub>.

### OSM-Dependent STAT3 Phosphorylation and SOCS3 Induction in Hepatocytes

Similar to IL-6, OSM stimulated STAT3 phosphorylation in isolated hepatocytes (Figure 4). The PGE<sub>2</sub>-dependent OSM production in Kupffer cells could thus be the basis for the induction of STAT3 phosphorylation in hepatocytes by supernatants of Kupffer cell cultures exposed to PGE<sub>2</sub>. In order to elucidate a possible interference between insulin and OSM signaling, hepatocytes were stimulated with 10 nM insulin subsequent to incubation with either IL-6 or OSM. Neither the IL-6-dependent nor the OSM-dependent STAT3 phosphorylation was affected by a subsequent stimulation of the hepatocytes with insulin.

IL-6 has previously been shown to interfere with insulin signaling in hepatocytes by inducing SOCS3 in a STAT3-dependent manner.<sup>10,12</sup> It was therefore tested whether OSM can induce SOCS3 formation in isolated hepatocytes. In line with expectations, OSM induced SOCS3 mRNA to a similar extent as a tenfold higher dose of IL-6 (Figure 5). Neither the IL-6-dependent nor the OSM-dependent induction of SOCS3 mRNA was affected by subsequent treatment with insulin.

Similar to Kupffer cells, OSM production was induced by PGE<sub>2</sub> in peritoneal macrophages (not shown). In hepatocytes, conditioned medium of PGE<sub>2</sub>-treated macrophages induced a stronger STAT3 phosphorylation and SOCS3 induction than conditioned medium from controls. If the

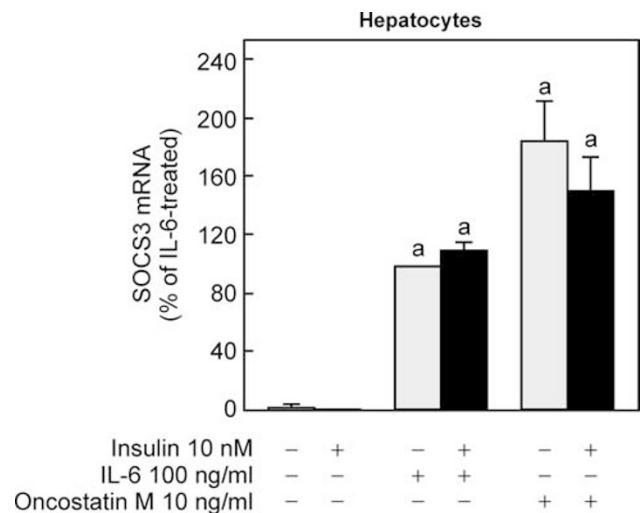


**Figure 5** SOCS3 induction by IL-6 and oncostatin M in rat hepatocytes. Rat hepatocytes were isolated and cultured as described in the legend to Figure 1. After a final medium change, they were incubated with IL-6 or oncostatin M for 330 min and subsequently without a further medium change with insulin for 120 min, as indicated. Cells were shock frozen, lysed in chaotropic buffer and SOCS3 mRNA was determined by RT real-time PCR with  $\beta$ -actin as reference gene. The SOCS3 mRNA level in IL-6-treated hepatocytes was set to 100%. Values are means  $\pm$  s.e.m. of four independent experiments. Statistics: Student's *t*-test for unpaired samples; <sup>a</sup>*P* < 0.05 versus control.

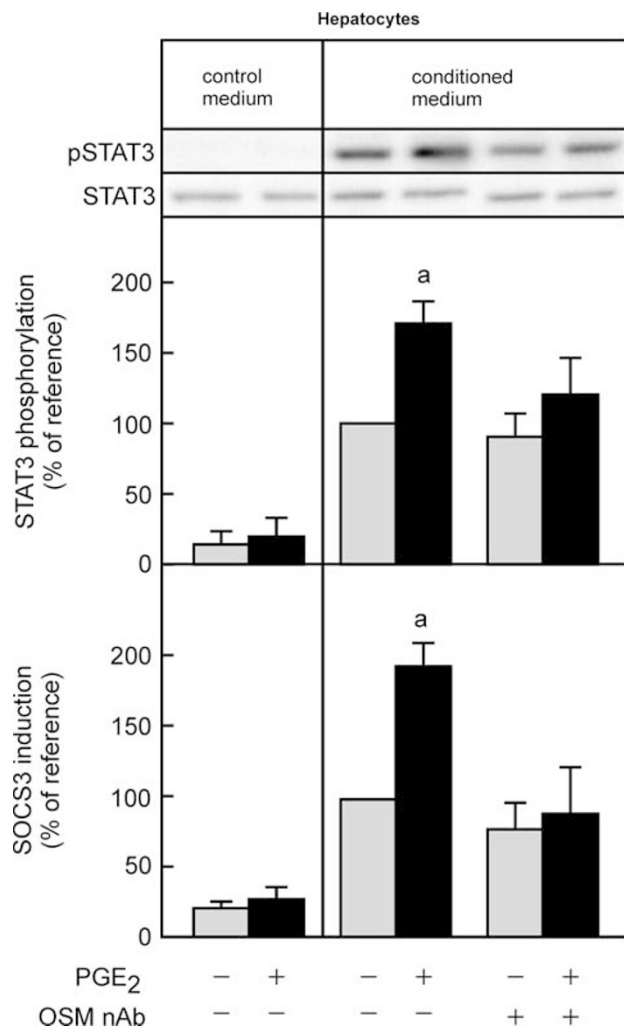


**Figure 6** Inhibition by a neutralizing anti-OSM antibody of STAT3 phosphorylation and SOCS3 induction in rat hepatocytes by conditioned media. Rat hepatocytes were isolated and cultured as described in the legend to Figure 1. After a final medium change, they were incubated for 6 h with control medium, medium containing 0.1  $\mu$ M PGE<sub>2</sub> or conditioned media of peritoneal macrophages cultured with or without 0.1  $\mu$ M PGE<sub>2</sub> for 24 h. Where indicated, conditioned medium was incubated with a neutralizing anti-OSM antibody before addition to hepatocytes. Hepatocytes were shock frozen and processed to analyze STAT3 phosphorylation or SOCS3 mRNA level as detailed in the Materials and methods section. pSTAT3/STAT3 ratio and SOCS3 mRNA level of hepatocytes treated with conditioned medium of control macrophages were set to 100%. Values are means  $\pm$  s.e.m. of four independent experiments. Statistics: Student's *t*-test for unpaired samples; <sup>a</sup>*P* < 0.05 versus control.

medium was incubated with an neutralizing anti-OSM antibody before stimulation of hepatocytes, the difference between conditioned medium of control cells and PGE<sub>2</sub>-treated macrophages was completely abolished (Figure 6).

#### In Vivo Relevance of the In Vitro Data

In order to elucidate whether the PGE<sub>2</sub>-dependent OSM production might be of relevance *in vivo* in a situation

similar to the metabolic syndrome, the hepatic expression of key regulatory enzymes of the prostanoid production and the expression of the cytokines IL-6 and OSM was determined in the course of the development of NAFLD in two different murine NAFLD models. Specimens of a previous animal experiment were used.<sup>14</sup> In one model, in which alterations closely resembling the (histo)pathophysiological changes observed in human NASH were induced,<sup>13</sup> steatosis as well as clear signs of inflammation developed (Figure 7), whereas the other model led to a similar degree of hepatic steatosis but without significant hepatic inflammation.<sup>14</sup> In the animal model showing histological signs of inflammation, both ALT and AST were significantly elevated, whereas only slightly and not significantly elevated ALT and AST levels were found in the steatosis model without histological signs of inflammation (Figure 7). At the time of killing, animals with steatotic livers had significantly elevated plasma glucose levels compared with the control group, whereas animals with signs of inflammation had similar plasma glucose levels as the controls (Figure 7).

As prostaglandins are not stored, prostaglandin levels depend on the rate of local production. Whereas (COX-1 is responsible for the prostaglandin production for most physiological processes, COX-2 in macrophages is induced during inflammation. As expected, COX-1 expression did not change very much in the course of the development of NASH. In contrast, COX-2 expression increased 50-fold in NASH livers (Figure 8). Notably, in livers with no apparent signs of inflammation, COX-2 was already induced approximately threefold.

Cytokine expression also increased in the course of NASH development. Thus, IL-6 mRNA levels were induced approximately fivefold in NASH livers. No induction of IL-6 was observed in livers with steatosis only (Figure 9). OSM mRNA was induced to a much larger extent than IL-6 mRNA. In NASH livers it was elevated approximately 30-fold in comparison with animals fed a control diet. Notably, OSM mRNA in contrast to IL-6 mRNA was already increased in livers of animals that had no apparent signs of inflammation (Figure 9).

In order to analyze the possible impact of the increased prostaglandin and OSM production on the development of insulin resistance and steatosis, the impact of OSM on insulin signaling in hepatocytes was studied.

#### Attenuation of Insulin-Dependent Akt Activation and Glucokinase Induction by OSM

Induction of SOCS3 has been shown to interrupt the insulin signal chain in hepatocytes. Therefore, it was tested whether OSM interfered with insulin signaling in hepatocytes. Stimulation of hepatocytes with insulin leads to an activation of the Akt kinase that can be monitored by the serine phosphorylation of the enzyme (Figure 10). In rat hepatocytes, insulin increased the ratio of phosphorylated Akt to total Akt approximately sevenfold. Previous incubation of the

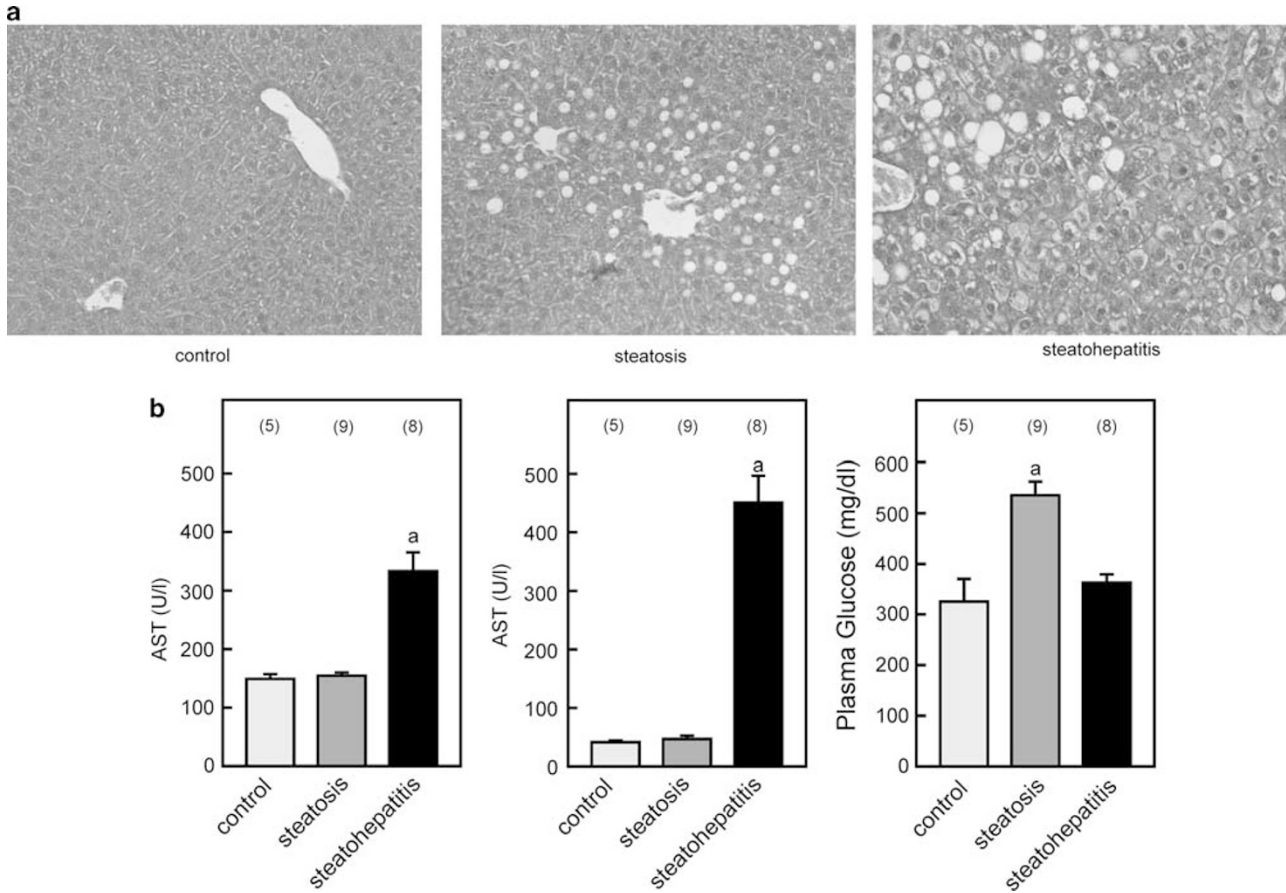


**Figure 7** Liver pathology and serum parameters of murine models of bland steatosis and steatohepatitis. Mice were fed either a high-fat diet leading to hepatic steatosis or a NASH-inducing diet for 12 weeks. Mice receiving standard chow served as control. (a) Liver histology. (b) Plasma samples were collected at the time of killing and AST, ALT and glucose were determined by standard assays. Values are means  $\pm$  s.e.m. of the number of animals indicated. Statistics: Student's *t*-test for unpaired samples, <sup>a</sup>*P* < 0.05.

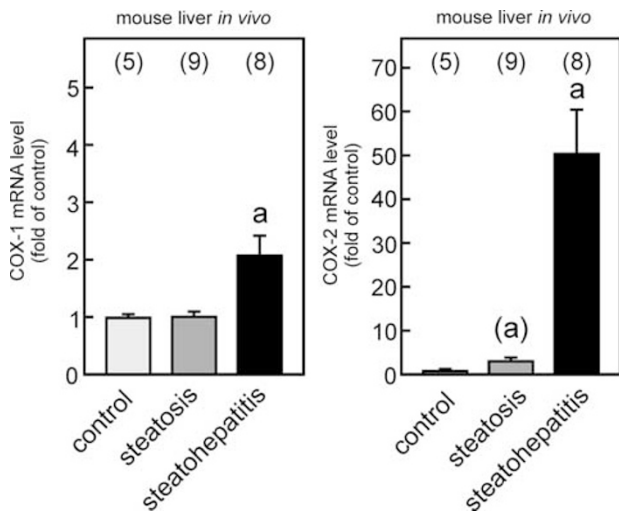


**Figure 8** Hepatic expression of cyclooxygenase 1 (COX-1) and cyclooxygenase 2 (COX-2) in murine models of bland steatosis and steatohepatitis. Mice were fed either a high-fat diet leading to hepatic steatosis or a NASH-inducing diet for 12 weeks. Mice receiving standard chow served as control. mRNA of COX-1 and COX-2 was determined by qPCR in snap-frozen liver samples taken at the end of the diet intervention. Values are means  $\pm$  s.e.m. of the number of animals indicated. Statistics: Student's *t*-test for unpaired samples, <sup>a</sup>*P* < 0.05; <sup>(a)</sup>*P* < 0.1.

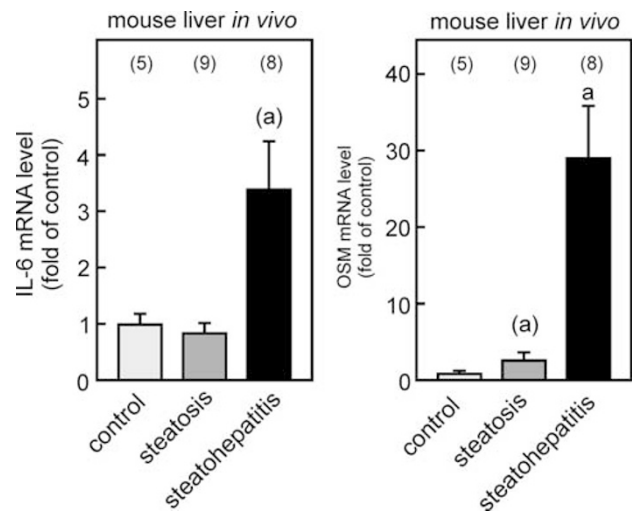


**Figure 9** Hepatic expression of the cytokines IL-6 and oncostatin M in murine models of bland steatosis and steatohepatitis. Mice were fed either a high-fat diet leading to hepatic steatosis or a NASH-inducing diet for 12 weeks. Mice receiving standard chow served as control. mRNA of IL-6 and OSM was determined by qPCR in snap-frozen liver samples taken at the end of the diet intervention. Values are means  $\pm$  s.e.m. of the number of animals indicated. Statistics: Student's *t*-test for unpaired samples, <sup>a</sup>*P* < 0.05; <sup>(a)</sup>*P* < 0.1.

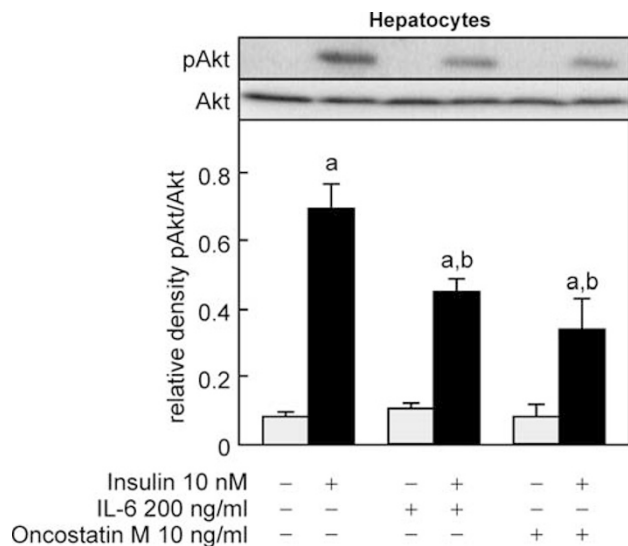


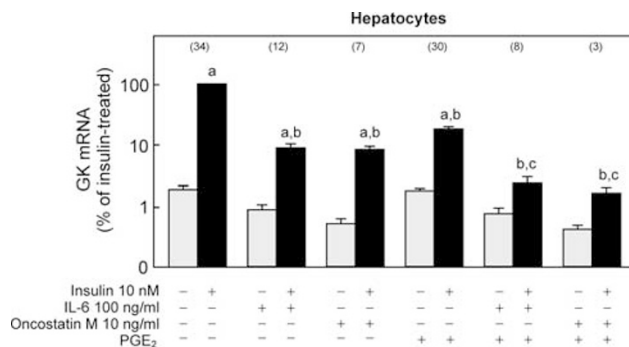
**Figure 10** Inhibition of the insulin-dependent phosphorylation of Akt by IL-6 and oncostatin M in rat hepatocytes. Rat hepatocytes were isolated and cultured as described in the legend to Figure 1. After a final medium change, they were incubated with IL-6 or oncostatin M for 330 min and subsequently without a further medium change with insulin for 60 min, as indicated. Cells were shock frozen, solubilized in lysis buffer and Akt phosphorylation was determined by western blot analysis with phospho-specific antibodies. Values are means  $\pm$  s.e.m. of three independent experiments. Statistics: Student's *t*-test for unpaired samples; <sup>a</sup>*P* < 0.05 versus control, <sup>b</sup>*P* < 0.05 versus insulin stimulated.

hepatocytes with IL-6 reduced the insulin-dependent Akt phosphorylation by approximately 30%. An even stronger reduction of the insulin-dependent Akt phosphorylation was observed after previous incubation of hepatocytes with OSM.

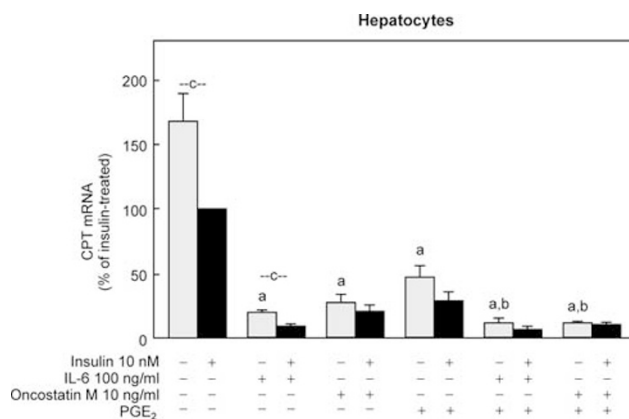
Activation of the Akt kinase results in the increase of the hepatocyte's capacity to utilize glucose. One of the key targets downstream of the Akt kinase is the induction of glucokinase, which is a key regulator in glycolysis as well as glycogen synthesis and glucose-dependent gene regulation in hepatocytes. Glucokinase mRNA was induced approximately 100-fold by insulin in rat hepatocytes (Figure 11). As reported previously, IL-6 reduced the insulin-dependent induction of GK mRNA by approximately 90%. A similar attenuation of the insulin-induced induction of GK mRNA was observed after incubation of hepatocytes with a tenfold lower concentration of OSM. Glucokinase induction was also attenuated by PGE<sub>2</sub>. Notably, PGE<sub>2</sub> further enhanced the IL-6- or the OSM-dependent attenuation of the insulin-dependent glucokinase induction.

### Impact of PGE<sub>2</sub> and OSM on Genes of Proteins Involved in Hepatic Lipid Metabolism

A decrease in hepatic glucose utilization could contribute to hyperglycemia but would rather protect the hepatocyte from steatosis, as the substrate for *de novo* liponeogenesis is not readily metabolized. However, lipid accumulation analyzed by oil red-staining occurred in hepatocytes treated with insulin, PGE<sub>2</sub>, and in OSM-treated cells (Supplementary Data,



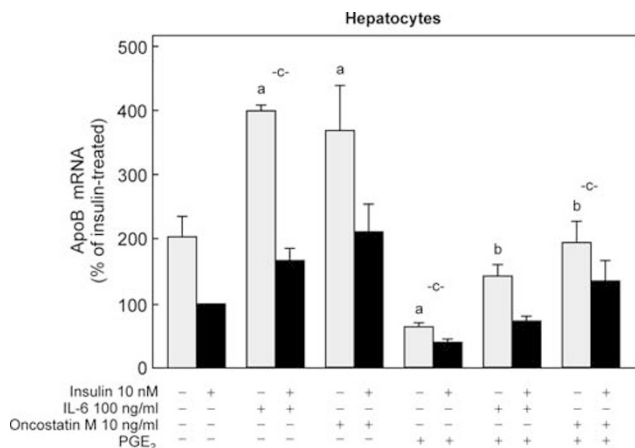
**Figure 11** Inhibition of the insulin-dependent glucokinase induction in rat hepatocytes by IL-6, oncostatin M and PGE<sub>2</sub>. Rat hepatocytes were isolated and cultured as described in the legend to Figure 1. After a final medium change, they were incubated with 100 ng/ml IL-6, 10 ng/ml oncostatin M and/or 10  $\mu$ M PGE<sub>2</sub> for 330 min and subsequently without a further medium change with insulin for 120 min, as indicated. Cells were shock frozen, lysed in chaotropic buffer and glucokinase (GK) mRNA was determined by RT real-time PCR with  $\beta$ -actin as reference gene. The GK mRNA level in insulin-treated hepatocytes was set to 100%. Values are means  $\pm$  s.e.m. of the number of independent experiments indicated. Note the log scale on the y-axis. Statistics: Student's *t*-test for unpaired samples; <sup>a</sup>*P* < 0.05 versus control, <sup>b</sup>*P* < 0.05 versus insulin treated, <sup>c</sup>*P* < 0.05 versus either stimulus alone.



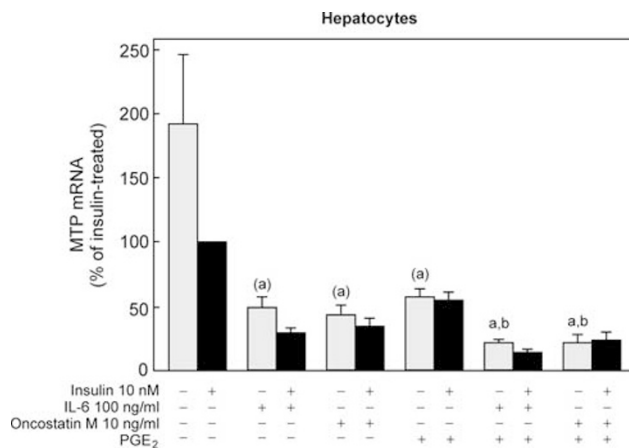
**Figure 12** Synergistic repression of CPT1 by PGE<sub>2</sub> and oncostatin M. Rat hepatocytes were isolated and cultured as described in the legend to Figure 9. After a final medium change, they were incubated with IL-6, oncostatin M and/or PGE<sub>2</sub> for 330 min and subsequently without a further medium change with insulin for 120 min, as indicated. Cells were shock frozen, lysed in chaotropic buffer and carnitine palmitoyl transferase 1 (CPT1) mRNA was determined by RT real-time PCR with  $\beta$ -actin as reference gene. The CPT1 mRNA level in insulin-treated hepatocytes was set to 100%. Values are means  $\pm$  s.e.m. of three independent experiments. Statistics: Student's *t*-test for unpaired samples; <sup>a</sup>*P* < 0.05 versus control; <sup>b</sup>*P* < 0.05 versus either stimulus alone; <sup>c</sup>*P* < 0.05 versus same treatment without insulin.

Figure S1). Triglyceride accumulation in hepatocytes not only depends on intrahepatic liponeogenesis but is also dependent on the rate of fatty acid oxidation and secretion of triglycerides from the hepatocyte into the plasma. A key regulatory enzyme in mitochondrial hepatic fatty acid oxidation is CPT1. CPT1 expression was decreased in response to insulin, IL-6, OSM and PGE<sub>2</sub> (Figure 12). Notably, CPT1 levels were





**Figure 13** Induction by OSM and IL-6 and repression by insulin and PGE<sub>2</sub> of apolipoprotein B (ApoB) expression. Rat hepatocytes were isolated and cultured as described in the legend to Figure 9. After a final medium change, they were incubated with IL-6, oncostatin M and/or PGE<sub>2</sub> for 330 min and subsequently without a further medium change with insulin for 120 min, as indicated. Cells were shock frozen, lysed in chaotropic buffer and ApoB mRNA was determined by RT real-time PCR with  $\beta$ -actin as reference gene. The ApoB mRNA level in insulin-treated hepatocytes was set to 100%. Values are means  $\pm$  s.e.m. of three independent experiments. Statistics: Student's *t*-test for unpaired samples; <sup>a</sup>*P* < 0.05 versus control; <sup>b</sup>*P* < 0.05 versus either stimulus alone; <sup>c</sup>*P* < 0.05 versus same treatment without insulin.



**Figure 14** Synergistic repression of MTP expression by OSM and PGE<sub>2</sub>. Rat hepatocytes were isolated and cultured as described in the legend to Figure 9. After a final medium change, they were incubated with IL-6, oncostatin M and/or PGE<sub>2</sub> for 330 min and subsequently without a further medium change with insulin for 120 min, as indicated. Cells were shock frozen, lysed in chaotropic buffer and microsomal triglyceride transfer protein (MTP) mRNA was determined by RT real-time PCR with  $\beta$ -actin as reference gene. The MTP mRNA level in insulin-treated hepatocytes was set to 100%. Values are means  $\pm$  s.e.m. of three independent experiments. Statistics: Student's *t*-test for unpaired samples; <sup>a</sup>*P* < 0.05 versus control; <sup>b</sup>*P* < 0.05 versus either stimulus alone; <sup>c</sup>*P* < 0.05 versus same treatment without insulin. Letters in parenthesis: significances for single-sided *t*-test.

lowest in cells treated with a combination of PGE<sub>2</sub> and either OSM or IL-6. In hepatocytes treated with IL-6, OSM and/or PGE<sub>2</sub>, the insulin-dependent regulation of CPT1 expression was attenuated.

Insulin, as previously reported, decreased ApoB expression in hepatocytes. PGE<sub>2</sub> decreased ApoB expression to a larger extent than insulin and appeared to enhance the insulin-dependent decrease in ApoB expression (Figure 13). In contrast, IL-6 induced the mRNA of ApoB. Similarly, OSM also induced ApoB mRNA. The induction by both cytokines was reduced by insulin and completely blunted in the presence of PGE<sub>2</sub>.

The lipidation of ApoB is strictly dependent on the presence of MTP. Insulin and IL-6 have previously been shown to decrease the expression of MTP. Whereas insulin caused a 50% reduction (Figure 14), IL-6 reduced MTP expression to approximately 25% of the control level. PGE<sub>2</sub> and OSM reduced the expression of MTP to a similar extent as IL-6. Notably, PGE<sub>2</sub> again enhanced the IL-6- or OSM-dependent repression of MTP.

## DISCUSSION

The current study showed that PGE<sub>2</sub> can stimulate OSM production in Kupffer cells (Figure 3). OSM released from Kupffer cells in response to PGE<sub>2</sub> may lead to a paracrine STAT3 phosphorylation in hepatocytes (Figures 1, 4 and 6), which results in an induction of SOCS3 (Figures 5 and 6). The same cascade appears to be triggered *in vivo* in the course of the development of NASH in mouse liver

(Figures 8 and 9). The OSM-dependent SOCS3 induction in hepatocytes may attenuate insulin-dependent Akt activation (Figure 10) and insulin-dependent induction of the key glycolytic enzyme glucokinase synergistically with PGE<sub>2</sub> (Figure 11). In addition, OSM and PGE<sub>2</sub> synergistically repressed the expression of enzymes critically involved in fatty acid oxidation (Figure 12) and triglyceride export from hepatocytes (Figures 13 and 14). Therefore, PGE<sub>2</sub> released locally from Kupffer cells in a state of chronic inflammation that often accompanies obesity might enhance hepatic insulin resistance and the development of hepatic steatosis both directly and by eliciting OSM release from Kupffer cells.

## Interplay of Cytokines and PGE<sub>2</sub>

PGE<sub>2</sub> influences the liver's response to inflammation in a complex manner: PGE<sub>2</sub> that is released from Kupffer cells in response to cytokines or bacterial endotoxins<sup>2</sup> has been shown to attenuate LPS-induced TNF- $\alpha$  production in Kupffer cells predominantly via activation of the EP4 receptor.<sup>6</sup> In addition, it attenuated the IL-6 production in Kupffer cells<sup>7,8</sup> and IL-6-dependent acute-phase response in hepatocytes,<sup>5</sup> as well as IL-6-dependent alterations of hepatic VLDL production.<sup>20</sup> These mechanisms contribute to a PGE<sub>2</sub>-dependent counter-regulation to an ongoing inflammation. However, in one study PGE<sub>2</sub> has been shown to enhance endotoxin-stimulated IL-6 production,<sup>9</sup> thereby augmenting the inflammatory response in a feed-forward loop. The stimulation by PGE<sub>2</sub> of OSM production in Kupffer cells described here also represents such a

proinflammatory feed-forward loop. The stimulation of OSM production in Kupffer cells is no isolated finding: PGE<sub>2</sub> has previously been shown to increase OSM production in astrocytes, monocytes and macrophages of murine and human origin.<sup>21</sup> The inflammatory feed-forward loop might be further bolstered by an OSM-dependent stimulation of PGE<sub>2</sub> production in Kupffer cells as it has been shown for other cell types.<sup>22</sup>

### Impact of PGE<sub>2</sub>-Dependent OSM Production on Insulin Resistance

We have previously shown that PGE<sub>2</sub> attenuated insulin signaling in rat hepatocytes by an EP3-R mediated activation of ERK1/2 that interrupted the intracellular signal chain by a serine phosphorylation of IRS.<sup>12</sup> PGE<sub>2</sub> synergized with IL-6, which also blunted insulin signaling in hepatocytes via an induction of SOCS3. The current results indicate that PGE<sub>2</sub> in addition to directly attenuating insulin signaling in hepatocytes can negatively affect insulin signaling also indirectly by eliciting OSM release from Kupffer cells. OSM in turn inhibited insulin signaling by a mechanism different from the direct action of PGE<sub>2</sub> on hepatocytes most likely similar to the mode of action of IL-6. The OSM-dependent attenuation of insulin signaling was additive to the direct attenuation of insulin signaling by PGE<sub>2</sub> in hepatocytes (Figure 11). The importance of such an indirect mode to induce insulin resistance is underlined by the recent finding that diet-induced hepatic insulin resistance can be blunted by previous functional elimination of Kupffer cells.<sup>11,23</sup> In addition, Kupffer cells might not be the sole source of OSM relevant for hepatic insulin resistance. OSM released in response to PGE<sub>2</sub> in macrophages in the intra-abdominal adipose tissue and peritoneal macrophages might be additional relevant sources. In line with this hypothesis, PGE<sub>2</sub> was able to elicit OSM formation in mouse peritoneal macrophages (J Henkel *et al*, unpublished observation).

### Impact of PGE<sub>2</sub>-Dependent OSM Production on Hepatic Steatosis

Steatosis of hepatocytes can be a result of increased liponeogenesis or decreased triglyceride export or fatty acid oxidation. Although PGE<sub>2</sub> inhibited insulin-induced fatty acid synthesis by attenuating signaling toward Akt kinase and hence the Akt-dependent induction and activation of enzymes involved in lipacidogenesis,<sup>24</sup> PGE<sub>2</sub> increased triglyceride accumulation in hepatocytes (Supplementary Figure S1). This was most likely because of inhibition of fatty acid and triglyceride consuming pathways independently of its interference with insulin signaling, which outweighed the inhibition of insulin-induced lipacidogenesis. In line with this preliminary observation, PGE<sub>2</sub> inhibited the expression of CPT1, the rate-controlling enzyme of mitochondrial  $\beta$ -oxidation synergistically with OSM. PGE<sub>2</sub> has been shown to inhibit  $\beta$ -oxidation in hepatocytes,<sup>25</sup> whereas OSM rather increased palmitate oxidation in HepG2 cells by inducing

acylCoA synthetase 3 and 5.<sup>26</sup> OSM, like IL-6, induced ApoB expression but at the same time repressed the expression of the microsomal transfer protein synergistically with PGE<sub>2</sub>. For IL-6 this has previously been shown to result in a defective VLDL production and an accumulation of triglycerides in the liver.<sup>20</sup> A similar mechanism can be assumed for OSM. Finally, SOCS3 induction in hepatocytes by OSM released in response to PGE<sub>2</sub> might favor fat accumulation in hepatocytes by yet another mechanism: induction of SOCS3 has been shown to be one of the mechanisms by which the hepatocyte can be rendered resistant to leptin signaling.<sup>27</sup> As a consequence, intrahepatic fatty acid metabolism is shifted from oxidation toward intrahepatic lipid accumulation.<sup>28,29</sup> The lipid accumulation itself might also contribute to hepatic insulin resistance.

### In Vivo Relevance

The potential *in vivo* relevance of the prostaglandin and OSM production in the development of NAFLD and insulin resistance is underscored by the findings in two mouse models of NAFLD (Figures 8 and 9). Notably, COX-2 and OSM mRNAs in contrast to IL-6 and TNF- $\alpha$ <sup>14</sup> mRNAs were already increased in livers with bland steatosis, indicating that the activation of this pathway is an early event that precedes overt inflammation. OSM belongs to the class of cytokines that use the common receptor subunit gp130 for signal transduction that activates the JAK/STAT pathway.<sup>30</sup> The prototypical member of this family is IL-6. There is controversial evidence for the role of IL-6 in the development of insulin resistance and hepatic steatosis. IL-6 levels are increased in obese patients and patients with NASH and *in vitro* experiments clearly show that IL-6 interferes with insulin signaling in hepatocytes, skeletal muscle cells and adipocytes.<sup>31</sup> Chronic exposure to IL-6 caused hepatic insulin resistance whereas depletion of IL-6 in an obese mouse model improved hepatic insulin action.<sup>32,33</sup> On the other hand, complete knockdown of hepatic gp130 signaling predisposed to rather than protected from the development of steatosis and insulin resistance in the liver.<sup>34</sup> Similarly, knockdown of IL-6 signaling with antibodies against the IL-6 receptor enhanced steatosis but reduced signs of inflammation in a mouse model of diet-induced NASH.<sup>35</sup> Systemic overexpression of IL-6 appears to enhance insulin sensitivity.<sup>36</sup> Although OSM belongs to the same class of cytokines as IL-6, no direct conclusion can be drawn from these studies as to the potential role of OSM in insulin resistance and steatosis. In contrast to IL-6, OSM cannot only signal via the common gp130 subunit but additionally through the OSM-receptor, which itself contains a signal transduction subunit and hence may activate cellular responses that differ from IL-6.<sup>30</sup> Therefore, the impact of OSM on the development of steatosis and insulin resistance in the liver may differ substantially from IL-6. Specific disruption of intrahepatic OSM signaling will be required to prove the hypothesis put forward here.

In summary, in addition to reducing hepatic insulin sensitivity by directly interrupting the insulin signal chain in hepatocytes, PGE<sub>2</sub> released from Kupffer cells or macrophages in tissues draining into the portal vein may contribute to hepatic insulin resistance by enhancing the OSM production in Kupffer cells and macrophages in an autocrine manner. OSM in turn may further reduce insulin sensitivity of hepatocytes in a SOCS3-dependent manner and propagate the development of hepatic steatosis. PGE<sub>2</sub>-dependent OSM formation and OSM signaling might be potential new targets in the treatment of hepatic insulin resistance and steatosis.

Supplementary Information accompanies the paper on the Laboratory Investigation website (<http://www.laboratoryinvestigation.org>)

#### ACKNOWLEDGEMENT

The excellent technical assistance of Manuela Kuna, Ines Kahnt and Christina Völker at the different stages of this work is gratefully acknowledged.

#### DISCLOSURE/CONFLICT OF INTEREST

The authors declare no conflict of interest.

- Tilg H, Moschen AR. Inflammatory mechanisms in the regulation of insulin resistance. *Mol Med* 2008;14:222–231.
- Kmiec Z. Cooperation of liver cells in health and disease. *Adv Anat Embryol Cell Biol* 2001;161:III–XIII, 1–151.
- Püschel GP, Jungermann K. Integration of function in the hepatic acinus: intercellular communication in neural and humoral control of liver metabolism. *Prog Liver Dis* 1994;12:19–46.
- Püschel GP, Christ B. Inhibition by PGE<sub>2</sub> of glucagon-induced increase in phosphoenolpyruvate carboxykinase mRNA and acceleration of mRNA degradation in cultured rat hepatocytes. *FEBS Lett* 1994;351:353–356.
- Fennekohl A, Lucas M, Püschel GP. Induction by interleukin 6 of G(s)-coupled prostaglandin E(2) receptors in rat hepatocytes mediating a prostaglandin E(2)-dependent inhibition of the hepatocyte's acute phase response. *Hepatology* 2000;31:1128–1134.
- Fennekohl A, Sugimoto Y, Segi E, *et al*. Contribution of the two Gs-coupled PGE<sub>2</sub>-receptors EP<sub>2</sub>-receptor and EP<sub>4</sub>-receptor to the inhibition by PGE<sub>2</sub> of the LPS-induced TNF $\alpha$ -formation in Kupffer cells from EP<sub>2</sub>-or EP<sub>4</sub>-receptor-deficient mice. Pivotal role for the EP<sub>4</sub>-receptor in wild type Kupffer cells. *J Hepatol* 2002;36:328–334.
- Goss JA, Mangino MJ, Callery MP, *et al*. Prostaglandin E<sub>2</sub> downregulates Kupffer cell production of IL-1 and IL-6 during hepatic regeneration. *Am J Physiol* 1993;264:G601–G608.
- Roland CR, Goss JA, Mangino MJ, *et al*. Autoregulation by eicosanoids of human Kupffer cell secretory products. A study of interleukin-1, interleukin-6, tumor necrosis factor- $\alpha$ , transforming growth factor- $\beta$ , and nitric oxide. *Ann Surg* 1994;219:389–399.
- Treffkorn L, Scheibe R, Maruyama T, *et al*. PGE<sub>2</sub> exerts its effect on the LPS-induced release of TNF- $\alpha$ , ET-1, IL-1 $\alpha$ , IL-6 and IL-10 via the EP<sub>2</sub> and EP<sub>4</sub> receptor in rat liver macrophages. *Prostaglandins Other Lipid Mediat* 2004;74:113–123.
- Senn JJ, Klover PJ, Nowak IA, *et al*. Interleukin-6 induces cellular insulin resistance in hepatocytes. *Diabetes* 2002;51:3391–3399.
- Neyrinck AM, Cani PD, Dewulf EM, *et al*. Critical role of Kupffer cells in the management of diet-induced diabetes and obesity. *Biochem Biophys Res Commun* 2009;385:351–356.
- Henkel J, Neuschäfer-Rube F, Pathe-Neuschäfer-Rube A, *et al*. Aggravation by prostaglandin E<sub>2</sub> of interleukin-6-dependent insulin resistance in hepatocytes. *Hepatology* 2009;50:781–790.
- Matsuzawa N, Takamura T, Kurita S, *et al*. Lipid-induced oxidative stress causes steatohepatitis in mice fed an atherogenic diet. *Hepatology* 2007;46:1392–1403.
- Dorn C, Riener MO, Kirovski G, *et al*. Expression of fatty acid synthase in nonalcoholic fatty liver disease. *Int J Clin Exp Pathol* 2010;3: 505–514.
- Hespling U, Jungermann K, Püschel GP. Feedback-inhibition of glucagon-stimulated glycogenolysis in hepatocyte/Kupffer cell cocultures by glucagon-elicited prostaglandin production in Kupffer cells. *Hepatology* 1995;22:1577–1583.
- Meredith MJ. Rat hepatocytes prepared without collagenase: prolonged retention of differentiated characteristics in culture. *Cell Biol Toxicol* 1988;4:405–425.
- Bradford MM. A rapid and sensitive method for the quantitation of microgram quantities of protein utilizing the principle of protein-dye binding. *Anal Biochem* 1976;72:248–254.
- Laemmli UK. Cleavage of structural proteins during the assembly of the head of bacteriophage T4. *Nature* 1970;227:680–685.
- Sobota RM, Muller PJ, Heinrich PC, *et al*. Prostaglandin E<sub>1</sub> inhibits IL-6-induced MCP-1 expression by interfering specifically in IL-6-dependent ERK1/2, but not STAT3, activation. *Biochem J* 2008;412: 65–72.
- Perez S, Aspichueta P, Ochoa B, *et al*. The 2-series prostaglandins suppress VLDL secretion in an inflammatory condition-dependent manner in primary rat hepatocytes. *Biochim Biophys Acta* 2006;1761:160–171.
- Repovic P, Benveniste EN. Prostaglandin E<sub>2</sub> is a novel inducer of oncostatin-M expression in macrophages and microglia. *J Neurosci* 2002;22:5334–5343.
- Repovic P, Mi K, Benveniste EN. Oncostatin M enhances the expression of prostaglandin E<sub>2</sub> and cyclooxygenase-2 in astrocytes: synergy with interleukin-1 $\beta$ , tumor necrosis factor- $\alpha$ , and bacterial lipopolysaccharide. *Glia* 2003;42:433–446.
- Huang W, Metlakunta A, Dedousis N, *et al*. Depletion of liver Kupffer cells prevents the development of diet-induced hepatic steatosis and insulin resistance. *Diabetes* 2010;59:347–357.
- Henkel J, Frede K, Püschel GP. Stimulation der hepatischen Lipidakkumulation durch PGE<sub>2</sub>-vermittelte Hemmung von  $\beta$ -Oxidation und VLDL-Bildung. *Z Gastroenterol* 2011;49:94.
- Brass EP, Alford CE, Garrity MJ. Inhibition of glucagon-stimulated cAMP accumulation and fatty acid oxidation by E-series prostaglandins in isolated rat hepatocytes. *Biochim Biophys Acta* 1987;930:122–126.
- Zhou Y, Abidi P, Kim A, *et al*. Transcriptional activation of hepatic ACSL3 and ACSL5 by oncostatin m reduces hypertriglyceridemia through enhanced beta-oxidation. *Arterioscler Thromb Vasc Biol* 2007;27:2198–2205.
- Uotani S, Abe T, Yamaguchi Y. Leptin activates AMP-activated protein kinase in hepatic cells via a JAK2-dependent pathway. *Biochem Biophys Res Commun* 2006;351:171–175.
- Tiniakos DG, Vos MB, Brunt EM. Nonalcoholic fatty liver disease: pathology and pathogenesis. *Annu Rev Pathol* 2010;5:145–171.
- Fabbrini E, Sullivan S, Klein S. Obesity and nonalcoholic fatty liver disease: biochemical, metabolic, and clinical implications. *Hepatology* 2010;51:679–689.
- Heinrich PC, Behrmann I, Haan S, *et al*. Principles of interleukin (IL)-6-type cytokine signalling and its regulation. *Biochem J* 2003;374:1–20.
- Allen TL, Febbraio MA. IL6 as a mediator of insulin resistance: fat or fiction? *Diabetologia* 2009;53:399–402.
- Klover PJ, Zimmers TA, Koniaris LG, *et al*. Chronic exposure to interleukin-6 causes hepatic insulin resistance in mice. *Diabetes* 2003;52:2784–2789.
- Klover PJ, Clementi AH, Mooney RA. Interleukin-6 depletion selectively improves hepatic insulin action in obesity. *Endocrinology* 2005;146:3417.
- Kroy DC, Beraza N, Tschaharganeh DF, *et al*. Lack of interleukin-6/glycoprotein 130/signal transducers and activators of transcription-3 signaling in hepatocytes predisposes to liver steatosis and injury in mice. *Hepatology* 2010;51:463–473.
- Yamaguchi K, Itoh Y, Yokomizo C, *et al*. Blockade of interleukin-6 signaling enhances hepatic steatosis but improves liver injury in methionine choline-deficient diet-fed mice. *Lab Invest* 2010;90: 1169–1178.
- Sadagurski M, Norquay L, Farhang J, *et al*. Human IL6 enhances leptin action in mice. *Diabetologia* 2009;53:525–535.